IHJPAS. 36 (3) 2023

Ibn Al-Haitham Journal for Pure and Applied Sciences
Journal homepage: jih.uobaghdad.edu.iq

Synthesis and Characterization Graphene- Carbon Nitride Nanostructure in One Step

Khalil Ibrahim Alabid*
Department of Chemistry ,Analytical Chemistry , Faculty of Science , Tishreen University ,Lattakia ,Syria.

Hajar Naser Nasser
Department of Chemistry ,Analytical Chemistry , Faculty of Science , Tishreen University ,Lattakia ,Syria.

***Coressponding Author:** khalilibrahimalabid@gmail.com

Article history: Received 11 November 2022, Accepted 30 March 2023, Published in July 2023.
doi.org/10.30526/36.3.3103

Abstract

Graphene-carbon nitride can be synthesized from thiourea in a single step at a temperature of four hours at a rate of 2.3 °C/min. Graphene-carbon nitride was characterized by Fourier-transform infrared spectroscopy (FTIR), energy dispersive X-ray analysis (EDX), scanning electron microscopy, and spectrophotometry (UV-VIS). Graphene-carbon nitride was found to consist of triazine and heptazine structures, carbon, and nitrogen. The weight percentage of carbon and the atomic percentage of carbon are 40.08%, and the weight percentage of nitrogen and the atomic percentage of nitrogen are 40.08%. Therefore, the ratio and the dimensions of the graphene-carbon nitride were characterized by scanning electron microscopy, and it was found that the radius was within the range of (2 µm-147.1 nm). In addition, it was found that it absorbed light in the visible field (VIS). The objective of the manufacture and characterization of graphene-carbon nitride for use in the manufacture of a selective electrode for an organic pollutant (currently used in the manufacture of a selective electrode for the analysis of organic dye).

Keywords: Graphene-Carbon Nitride, Structural characterization, Carbon Sheets, Polymer, Thermal method.

1. Introduction

Increasing interest in the field of nanotechnology, especially graphene and graphene-carbon nitride $g-C_3N_4$ is due to their interesting electrical, thermal, and mechanical properties. Graphene-carbon nitride $g-C_3N_4$ is a two-dimensional sheet(2D) [1-2] Metal-free [3-6], and semiconductor [7]. Band gaps are (2.7 eV) [8-9], hybridization sp^2- hybridized [10] and $\pi-$ conjugated [11] . Graphene-carbon nitride $g-C_3N_4$ can be prepared from several materials in the presence of temperature: melamine [12-13], dicyandiamide [14-15], trithiocyanuric acid [16-17], urea [18-21], thiourea [22-23], cyanamide [24], as shown in **Figure1**:

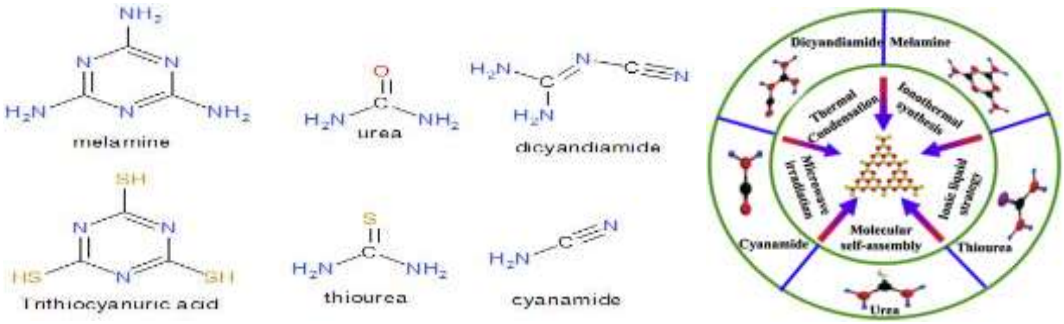

Figure 1. Materials that can be used in the synthesis for $g-C_3N_4$

Graphene-carbon nitride $g-C_3N_4$ is used in many applications, including: solar cells [25-26], super-capacitors [27-28], energy storage [29-30], and in the manufacture of electrochemical sensors, such as the mercury sensor [31]. The nitro sensor NO_X [32], the hydrogen sulfide sensor H_2S [33], which is sensitive to silver ions Ag^+[34]. It is also used in fuel cells [35-36], the pharmaceutical and medical sides [37-38]. Recently, many studies have focused on the optical applications of $g-C_3N_4$ photo catalytic applications [39-44]. The $g-C_3N_4$ can be used in the removal and dissolution of many organic pollutants [45-47], also used to remove CO_2 gas from the air [48]. Recently, the $g-C_3N_4$ is used to generate hydrogen and oxygen from water according to the following potentials and equations (1-2-3) [49]:

Full reaction: $2H_2O_{(l)} \rightarrow O_{2(g)} + H_{2(g)}$ $\Delta E^0 = 1.23\ V.(1)$

Half-reaction: Oxidation reaction: $2H_2O_{(l)} \rightarrow O_{2(g)} + 4H^+(aq) + 4e^-$ $\Delta E^0 = 1.23\ V\ vs.SHE(2)$

Reduction reaction: $4H^+(aq) + 4e^- \rightarrow 2H2(g)$ $\Delta E^0 = 0.00\ V\ vs.SHE(3)$

is the equilibrium potential under the standard conditions and SHE is the standard hydrogen electrode E^0

The $g-C_3N_4$ is a semiconductor used to increase its effectiveness. It is mixed with other materials; this doping is a suitable and effective technique to modify the band gap reducing the resistance of the large interface layer, enhancing the photocatalytic activity of $g-C_3N_4$ and removing to improve its properties as well. One of the strategies to improve the band gap, and enhance the photo catalytic activity of graphene-carbon nitride is to add doping, as shown in **figure 2** [50].

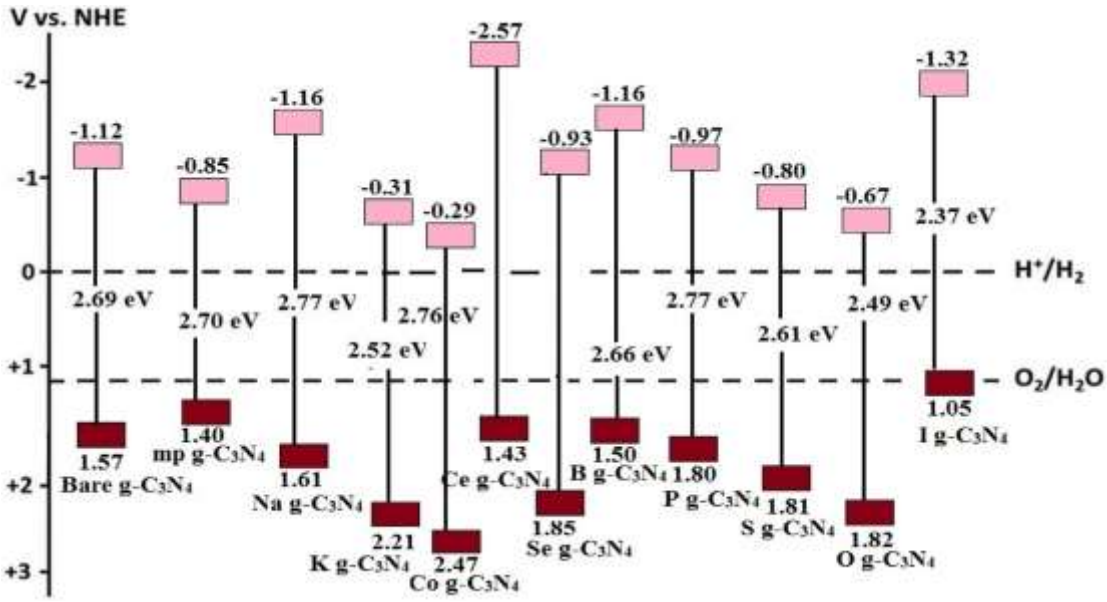

Figure 2. Band gap positioning with respect to conduction and valence band potentials of bare $g-C_3N_4$ and non-precious metal doped $g-C_3N_4$

The formation of $g-C_3N_4$ from its materials depends on time and temperature affects the spacing of the graphene-carbon nitride layers from each other, as in **Figure 3**:

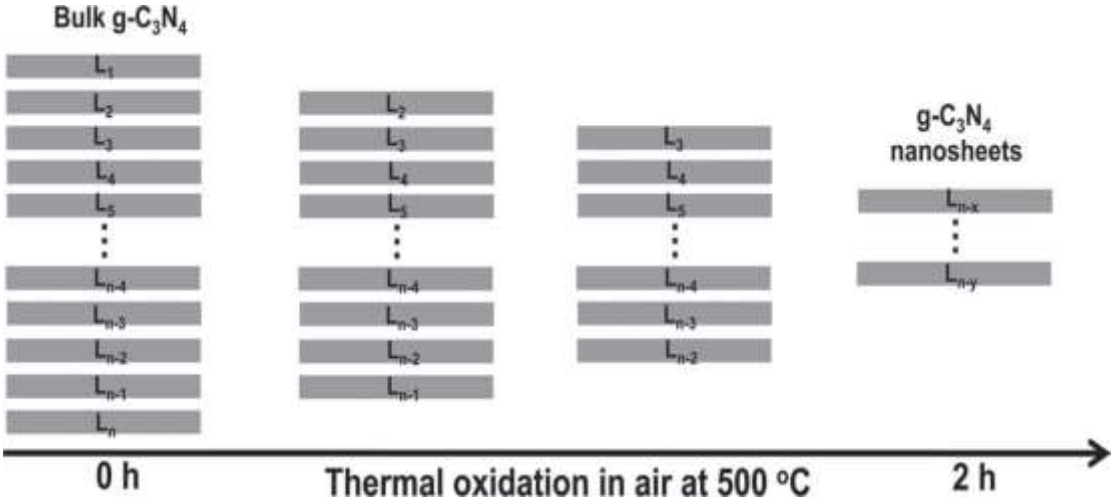

Figure 3. A schematic diagram of the formation of $\boldsymbol{g-C_3N_4}$ nanosheets and their thermal effect at $\mathbf{500}$ ℃ in air [51].

To confirm the fabrication of graphene-carbon nitride, measurements are done by fourier-transform infrared spectroscopy (FTIR), [52-64] and energy dispersive x-ray analysis (EDX) [65-68]. The objective of the manufacture is at 580 ℃ degrees, which is a critical point for its manufacture.

The objective of the manufacture and characterization of graphene-carbon nitride is performed for use in the manufacture of a selective electrode for an organic pollutant, (currently it is used in the manufacture of a selective electrode for the analysis of organic dye).

2. Chemical, instruments and method

The chemicals used in this research are high-purity materials: thiourea CH_4N_2S, thermal furnace (CARBOLITE), energy dispersive X-ray analysis (EDX), which is company namel; EDAX, scanning electron microscopy (SEM), which is a company name; TESCAN model VEGA II Xmu; spectrophotometer (UV-VIS) D-Lab model SP-UV1000; Fourier-transform infrared spectroscopy (FTIR); Balance Sartorius type TE64, porcelain crucible; and agate mortar.

Graphene-carbon nitride $g-C_3N_4$ is made by an easy, one-step method, through the direct polymerization process of thiourea, approximately 5.0016 g of thiourea is placed in a covered crucible of 50 ml, and then heated at 580 ℃ for 4 h in a muffle furnace. The temperature is gradually increased at a rate of 2.3 ℃$/min,$ and then left to cool to reach the temperature of the laboratory. Then it is ground in an agate mortar, and we get a yellow powder, as in **Figure 4**. When it is manufactured at 580 ℃ which is a critical point for its manufacture, when the temperature 600 ℃, it is noted that there is disappearance in the porcelain crucible, which denotes the decomposition of thiourea.

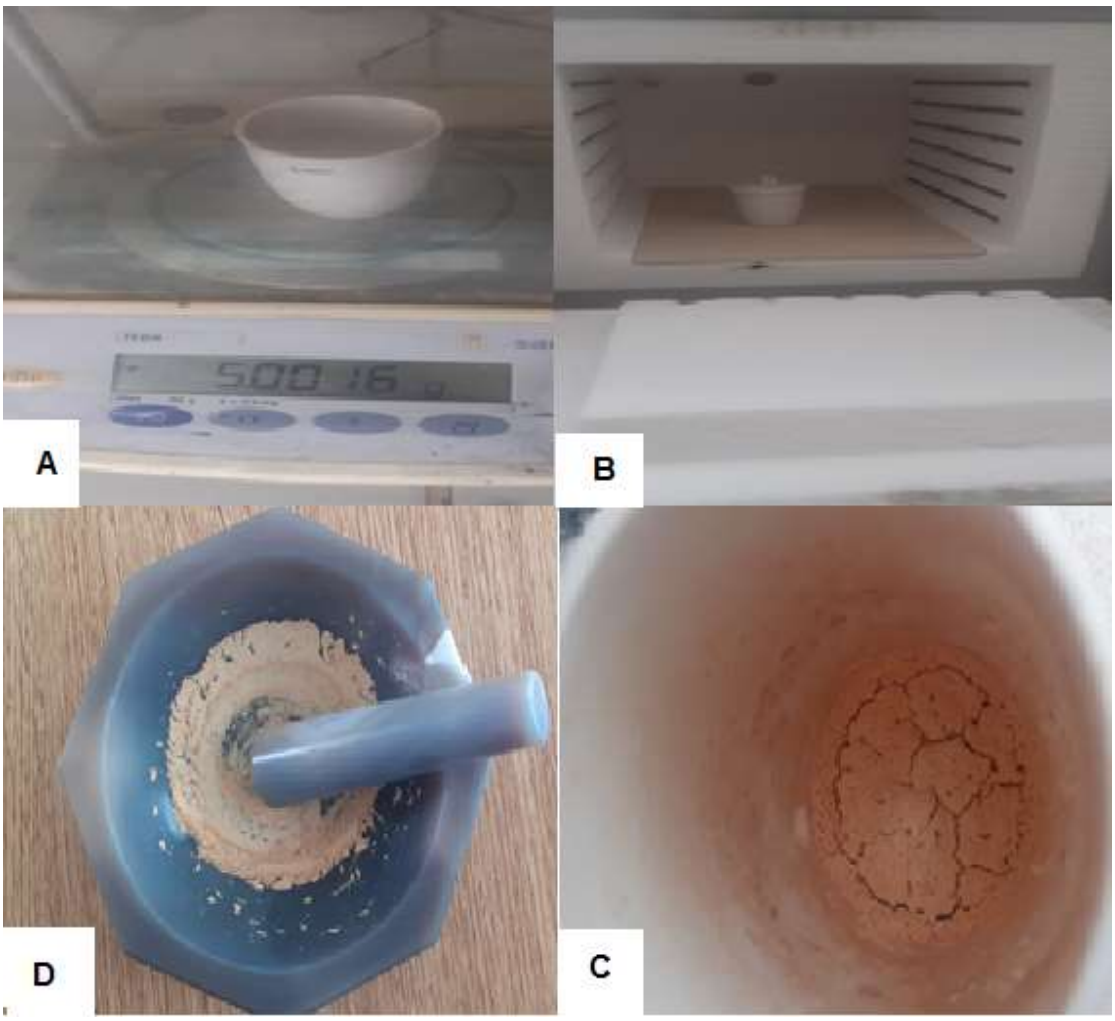

Figure 4. Photographs of the formation stages of carbon nitride sheets $g-C_3N_4$ A) Thiourea weight B) incineration at a temperature of 580 °C for four hours at a rate of 2.3 °C/min C) after cooling D) grinding the product in an agate mortar

3. Results and Discussion:

The graphene carbon nitride $g-C_3N_4$ was characterized using FTIR spectroscopy based on molecular vibration within the range of $(500-4000)\ cm^{-1}$ shown in **Figure 5.**

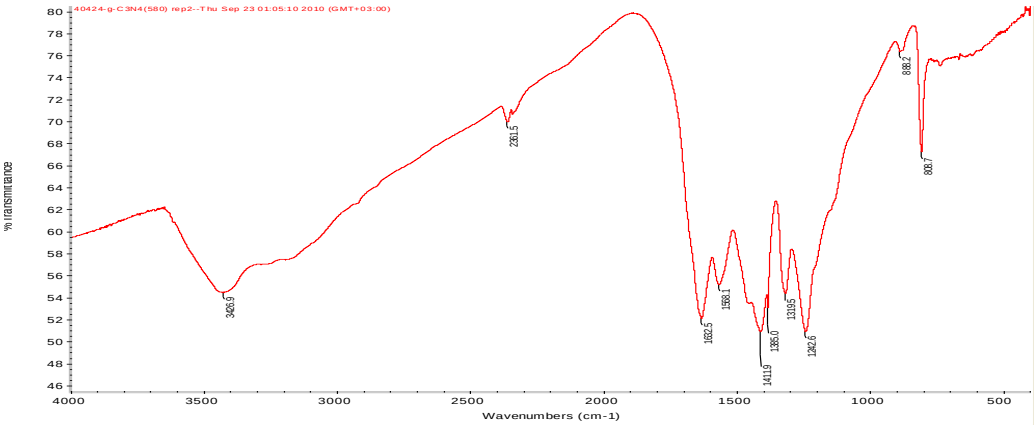

Figure 5. FTIR Spectroscopy for $g-C_3N_4$

Peaks at 808.7 $cm^{-1}$and 888.2 cm^{-1} correspond to the presence of s-triazine in $g-C_3N_4$. This bending is caused by the vibration of the tri-s-triazine (heptazine) ring. The peaks from 1242.6 cm^{-1} to 1632.5 cm^{-1} are attributed to the expansion vibration of the heterocyclic

aromatic C_6N_7 heptazine. Peaks are observed at 1319.5 cm^{-1}, 1385.0 cm^{-1}, 1411.9 cm^{-1}, and 1568.1cm^{-1} sticking together due to stretching vibrations of the $C-N$ bonds, while a peak appears at 1632.5 cm^{-1} related to the expansion vibration of the $C-N$ bond with heptazine units. Peaks between 900 cm^{-1} and 1800 cm^{-1} are attributed to the trigonal $C-N(-C)-C$ or $C-NH-C$ in ring. The absorption band centered at 3426.9 cm^{-1} corresponds to the vibrational stretching of the $N-H$ bond which denotes the presence of NH and NH_2 groups at edges in the $g-C_3N_4$. The broad peaks between 3000 cm^{-1} and 3500cm^{-1} are contributed by the lengthening of N –H [52-64]. So, graphene-carbon nitride is consisted the triazine and tri-s-triazine (heptazine) [69-74], as in **Figure 6**.

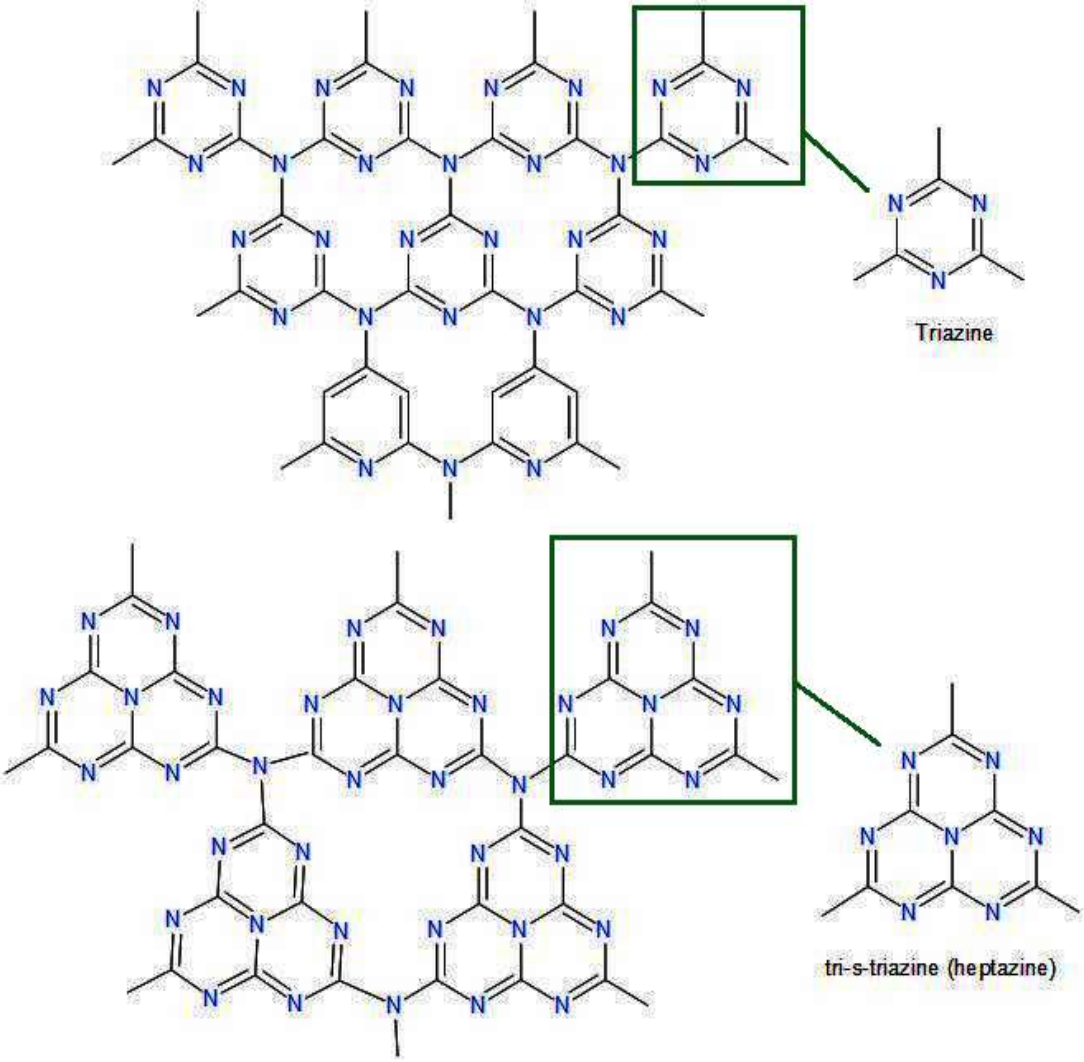

Figure 6. Tri-s-triazine (heptazine) and triazine structures of $\boldsymbol{g-C_3N_4}$

The process of manufacturing $g-C_3N_4$ depends on the formation of a polymer from thiourea after exposure to temperature, as is shown in **Figure 7.**

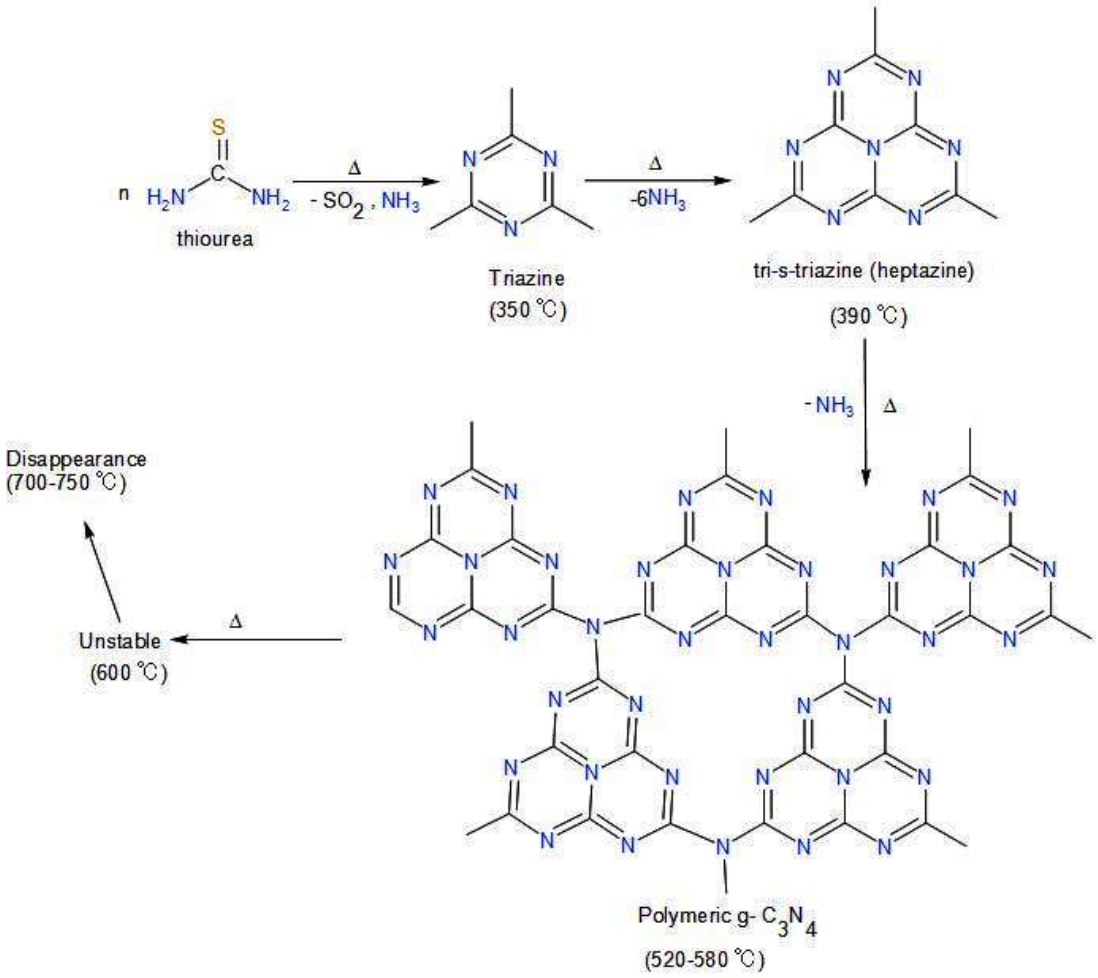

Figure 7. The stages of $\boldsymbol{g-C_3N_4}$ polymerization from thiourea

The $g-C_3N_4$ is characterized by energy dispersive X-ray analysis (EDX) as in table (1) and **Figure 8** :

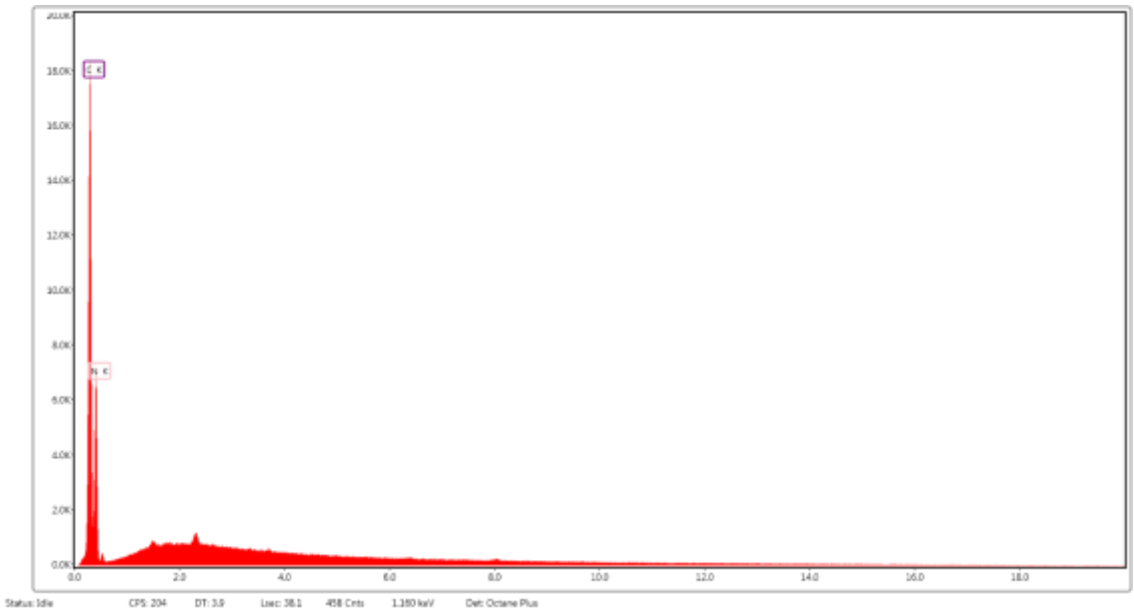

Figure 8. spectrum for $\boldsymbol{g-C_3N_4}$ by (EDX)

Table1. Elemental analysis $g-C_3N_4$ by energy dispersive X-ray analysis (EDX)

Element	Weight	Atomic	Error	Net Int.	K Ratio	Z	R	A	F	
C K	36.45%	40.08%	3.77%	2795.78	0.2654	1.0132	0.9936	0.719		1
N K	63.55%	59.92%	9.85%	1065.86	0.0854	0.9921	1.0035	0.1356		1

The energy dispersive X-ray analysis (EDX) showed that there is a peak at $0.27keV$ indicating the presence of $C-K$ carbon, and a peak at 0.39 keV indicating the presence of N-K nitrogen, the weight percentage of carbon is 36.45 %, and the atomic percentage of carbon is 40.08%, and the weight percentage of nitrogen is 63.55 %, and the atomic percentage of nitrogen is 59.92 %, so the ratio is 3 C and 4 N .The $g-C_3N_4$ is characterized using scanning electron microscopy (SEM) as shown in **Figure 9** .

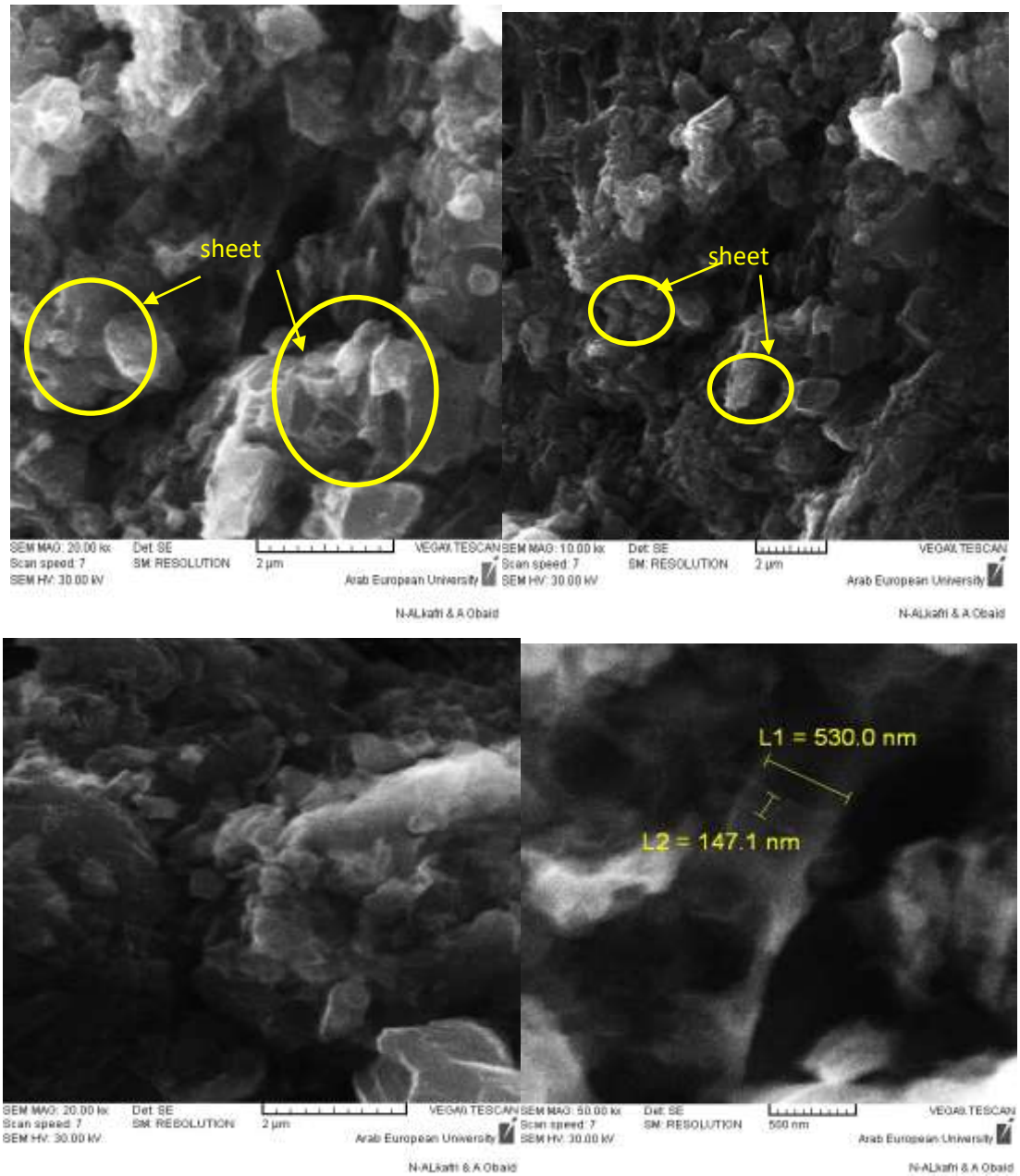

Figure 9. SEM scanner for $g-C_3N_4$

From the SEM scanning and using the Image J program, it is found that the shape is $g - C_3N_4$ graphene-carbon nitride sheets, which are lamellar interfaces (sheet) with a radius within the range of (2 µm -147.1 nm).

The optical spectrum is studied for the graphene - carbon nitride g-C_3N_4 sheets, as shown in **Figure 10**:

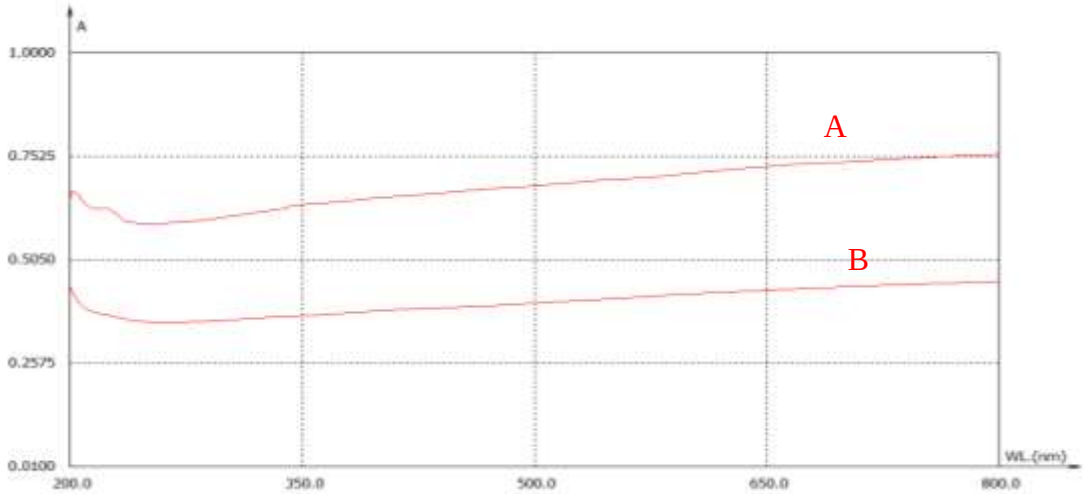

Figure 10. Scanning spectrum of 0.005 g/5ml of $g - C_3N_4$
The solution is absolute A) ethanol B) distilled water

It is noted that $g - C_3N_4$ is not soluble in solutions (water - ethanol) and it has a superior ability to absorb visible light $g - C_3N_4$ [8,9]. This is due to its band gap of 2.7 eV [8, 9, 75] by spectrophotometry

4. Conclusion

Graphene-carbon nitride can be synthesized from thiourea in a single-step. Graphene-carbon nitride is characterized. It is found to consists of triazine and heptazine structures. It also consists of carbon and nitrogen. The atomic percentage of carbon is 40.08%, and the atomic percentage of nitrogen is 59.92 %, so the ratio is $3C$ and $4N$. The dimensions of the graphene-carbon nitride are characterized by (SEM) , and it is found that the radius is within the range of (2 µm- 147.1 nm).

References:

1. Ong, W. J.; 2D/2D graphitic carbon nitride heterojunction nanocomposites for photocatalysis: why does face-to-face interface matter?. Frontiers in Material**, 2017,** s, *4*, 11.
2. Zhang, Z.; Jiang, D.; Li, D.; He, M.; Chen, M.. Construction of SnNb2O6 nanosheet nanosheet two-dimensional heterostructures with improved photocatalytic activity: synergistic effect and mechanism insight. Applied Catalysis B: Environmental, **2016,** *183*, 113-123.
3. Starukh, H.; Praus, P.. Doping of graphitic carbon nitride with non-metal elements and its applications in photocatalysis. Catalysts, **2020,** *10,2019*
4. Dong, G.; Zhang, Y.; Pan, Q.; Qiu, J. A fantastic graphitic carbon nitride material: electronic structure, photocatalytic and photoelectronic properties. Journal of Photochemistry and Photobiology C: Photochemistry Reviews, **2014,** *20*, 33-50.
5. Bai, L.; Huang, H.; Zhang, S.; Hao, L.; Zhang, Z.; Li, H.; Zhang, Y. Photocatalysis-Assisted Co3O4/g-C3N4 p–n Junction All-Solid-State Supercapacitors: A Bridge between Energy Storage and Photocatalysis. Advanced Science, **2020,** *7*, *22*,, 2001939.

6. Shi, M.; Xiao, P.; Lang, J.; Yan, C.; Yan, X. Porous g-C3N4 and MXene dual-confined FeOOH quantum dots for superior energy storage in an ionic liquid. Advanced Science, **2020,** *7, 2,*, 1901975.

7. Hayat, A.; Al-Sehemi, A. G.; El-Nasser, K. S.; Taha, T. A.; Al-Ghamdi, A. A.; Syed, J. A. S.; Nawawi, W. I.. Graphitic carbon nitride (g–C3N4,–based semiconductor as a beneficial candidate in photocatalysis diversity. *International Journal of Hydrogen Energy***, 2021**.

8. Yang, Z.; Xing, Z.; Feng, Q.; Jiang, H.; Zhang, J.; Xiao, Y.; Zhou, W.. Sandwich-like mesoporous graphite-like carbon nitride (Meso-g-C3N4)/WP/Meso-g-C3N4 laminated heterojunctions solar-driven photocatalysts. *Journal of colloid and interface science*, **2020,** *68*, 255-263.

9. Hu, T.; Dai, K.; Zhang, J.; Zhu, G.; Liang, C.. One-pot synthesis of step-scheme Bi2S3/porous g-C3N4 heterostructure for enhanced photocatalytic performance. *Materials Letters*, **2019,** *257*, 126740.

10. Mohamed, M. A.; Zain, M. F. M.; Minggu, L. J.; Kassim, M. B.; Amin, N. A. S.; Salleh, W. N. W.; Hir, Z. A. M. Constructing bio-templated 3D porous microtubular C-doped g-C3N4 with tunable band structure and enhanced charge carrier separation. Applied Catalysis B: *Environmental*, **2018,** 236, 265-279.

11. Xiong, T.; Cen, W.; Zhang, Y.; Dong, F. Bridging the g-C3N4 interlayers for enhanced photocatalysis. Acs Catalysis, **2016,** *6,4*, 2462-2472.

12. Gashi, A.; Parmentier, J.; Fioux, P.; Marsalek, R. Tuning the C/N Ratio of C-Rich Graphitic Carbon Nitride (g-C3N4) Materials by the Melamine/Carboxylic Acid Adduct Route. *Chemistry–A European Journal*, **2022,** *28,14*, e202103605.

13. Yi, Y.; Wang, J.; Niu, Y.; Yu, Y.; Wu, S.; Ding, K. Exploring the evolution patterns of melem from thermal synthesis of melamine to graphitic carbon nitride. RSC Advances,**2022,** *12,37*, 24311-24318.

14. Yao, G.; Liu, Y.; Liu, J.; Xu, Y. Facile Synthesis of Porous g-C3N4 with Enhanced Visible-Light Photoactivity. *Molecules*, **2022,** *27 ,6*, 1754.

15. Wang, J.; Yin, S.; Zhang, Q.; Cao, F.; Xing, Y.; Zhao, Q.; Wu, M. Single-Atom Fe-N4 sites promote the triplet-energy transfer process of g-C3N4 for the photooxidation. Journal of Catalysis, **2021,** *404*, 89-95.

16. Jia, Z.; Zhang, H.; Yu, Y.; Chen, Y.; Yan, J.; Li, X.; Zhang, H.. Trithiocyanuric acid derived g–C3N4 for anchoring the polysulfide in Li–S batteries application. *Journal of Energy Chemistry*, **2020,** *43*, 71-77.

17. Guan, K.; Li, J.; Lei, W.; Wang, H.; Tong, Z.; Jia, Q.; Zhang, SSynthesis of sulfur doped g-C3N4 with enhanced photocatalytic activity in molten salt. *Journal of Materiomics*,**2021,** *7 ,5*, 1131-1142.

18. Hu, C.; Chu, Y. C.; Lin, Y. R.; Yang, H. C.; Wang, K. H. Photocatalytic dye and Cr (VI) degradation using a metal-free polymeric g-C3N4 synthesized from solvent-treated urea. *Polymers*, **2019,** *11* ,1, 182.

19. Tapo, A.; Busabok, C.; Sujaridworakun, P.; Ngernchuklin, P.; influence of air and nitrogen atmosphere on g-C3N4 synthesized from urea. Khongwong, *WThai Journal of Nanoscience and Nanotechnology*, **2022,** *7* ,1.

20. Khan, M. E.; Khan, M. M.; Cho, M. H.. Environmentally sustainable biogenic fabrication of AuNP decorated-graphitic gC3N4 nanostructures towards improved photoelectrochemical performances. RSC advances, **2018,**8,25, 13898-13909.

21. Wen, J.; Xie, J.; Chen, X.; Li, X. A review on g-C3N4-based photocatalysts. *Applied surface science*, **2017,** *391*, 72-123.

22. Hong, Y.; Liu, E.; Shi, J.; Lin, X.; Sheng, L.; Zhang, M.;Chen, J.. A direct one-step synthesis of ultrathin g-C3N4 nanosheets from thiourea for boosting solar photocatalytic H2 evolution. *international journal of hydrogen energy*, **2019,** *44 ,14*, 7194-7204.

23. Bhat, S. S.; Jun, S. E.; Lee, S. A.; Lee, T. H.; Jang, H. W.. Influence of C3N4 precursors on photoelectrochemical behavior of TiO2/C3N4 photoanode for solar water oxidation. *Energies*, **2020,** *13*,4, 974.

24. Piao, H.; Choi, G.; Jin, X.; Hwang, S. J.; Song, Y. J.; Cho, S. P.; Choy, J. H. Monolayer Graphitic Carbon Nitride as Metal-Free Catalyst with Enhanced Performance in Photo-and Electro-Catalysis. Nano-micro letters, **2022,** *14 ,1*, 1-14.

25. Gkini, K.; Martinaiou, I.; Falaras, P. A Review on Emerging Efficient and Stable Perovskite Solar Cells Based on g-C3N4 Nanostructures. Materials, **2021,** *14 ,7*, 1679.

26. Yang, X.; Zhao, L.; Wang, S.; Li, J.; Chi, B. Recent progress of g-C3N4 applied in solar cells. Journal of Materiomics, **2021,** *7,4*, 728-741.

27. Ragupathi, V.; Panigrahi, P.; Subramaniam, N. G. g-C3N4 doped MnS as high performance electrode material for supercapacitor application. Materials Letters, **2019,** *246*, 88-91.

28. Thiagarajan, K.; Bavani, T.; Arunachalam, P.; Lee, S. J.; Theerthagiri, J.; Madhavan, J.; Choi, M. Y. Nanofiber NiMoO4/g-C3N4 composite electrode materials for redox supercapacitor applications. Nanomaterials, **2020,** *10,2*, 392.

29. Ngo, Y. L. T.; Chung, J. S.; Hur, S. H. Multi-functional NiO/g-C3N4 hybrid nanostructures for energy storage and sensor applications. Korean Journal of Chemical Engineering, **2020,***37 ,9*, 1589-1598.

30. Liu, P.; Zhang, Z.; Hao, R.; Huang, Y.; Liu, W.; Tan, Y.; Liu, K. Ultra-highly stable zinc metal anode via 3D-printed g-C3N4 modulating interface for long life energy storage systems. *Chemical Engineering Journal*, **2021,** *403*, 126425

31. Zhang, J.; Zhu, Z.; Di, J.; Long, Y.; Li, W.; Tu, Y. A sensitive sensor for trace Hg2+ determination based on ultrathin g-C3N4 modified glassy carbon electrode. Electrochimica Acta, **2015,.** 186, 192-200.

32. Cai, Z.; Chen, J.; Xing, S.; Zheng, D.; Guo, L. Highly fluorescent g-C3N4 nanobelts derived from bulk g-C3N4 for NO2 gas sensing. *Journal of Hazardous Materials*, **2021,** *416*, 126195.

33. Zeng, B.; Zhang, L.; Wan, X.; Song, H.; Lv, Y. Fabrication of α-Fe2O3/g-C3N4 composites for cataluminescence sensing of H2S. Sensors and Actuators B: Chemical**,2015**, 211, 370-376.

34. Alizadeh, T.; Rafiei, FAn innovative application of graphitic carbon nitride ,g-C3N4) nano-sheets as silver ion carrier in a solid state potentiometric sensor. *Materials Chemistry and Physics*, **2019,** *227*, 176-183.

35. Yuda, A.; Kumar, A. A review of g-C3N4 based catalysts for direct methanol fuel cells. *International Journal of Hydrogen Energy*,**2021.**

36. Liu, Q.; Zhang, JGraphene supported Co-g-C3N4 as a novel metal–macrocyclic electrocatalyst for the oxygen reduction reaction in fuel cells. Langmuir, **2013,***29 ,11*, 3821-3828

37. Li, X.; Yuan, Y.; Pan, X.; Zhang, L.; Gong, J. Boosted photoelectrochemical immunosensing of metronidazole in tablet using coral-like g-C3N4 nanoarchitectures. Biosensors and Bioelectronics, **2019,** *123*, 7-13.

38. Thurston, J. H.; Hunter, N. M.; Wayment, L. J.; Cornell, K. A. Urea-derived graphitic carbon nitride, (g-C3N4) films with highly enhanced antimicrobial and sporicidal activity. *Journal of colloid and interface science*, **2017,** *505*, 910-918.

39. Zhao, X.; Zhang, Y.; Zhao, X.; Wang, X.; Zhao, Y.; Tan, H.; Li, Y. Urea and melamine formaldehyde resin-derived tubular g-C3N4 with highly efficient photocatalytic performance. ACS applied materials interfaces, **2019,** *11 ,31*, 27934-27943.

40. Chidhambaram, N.; Ravichandran, K. Single step transformation of urea into metal-free g-C3N4 nanoflakes for visible light photocatalytic applications. Materials Letters, **,2017,** *207*, 44-48.

41. Khan, M. E.; Han, T. H.; Khan, M. M.; Karim, M. R.; Cho, M. H. Environmentally sustainable fabrication of Ag@ g-C3N4 nanostructures and their multifunctional efficacy as antibacterial agents and photocatalysts. ACS Applied Nano Materials, **2018,** *1,6*, 2912-2922.

42. Reddy, K. R.; Reddy, C. V.; Nadagouda, M. N.; Shetti, N. P.; Jaesool, S.; Aminabhavi, T. M. Polymeric graphitic carbon nitride ,(g-C3N4)-based semiconducting nanostructured materials: synthesis methods, properties and photocatalytic applications. *Journal of environmental management*, **2019,** *238*, 25-40.

43. Iqbal, N. ; Tailoring g-C3N4 with Lanthanum and Cobalt Oxides for Enhanced Photoelectrochemical and Photocatalytic Activity. Catalysts**, 2021**, *12 ,1*, 15.

44. Ye, L.; Chen, S. Fabrication and high visible-light-driven photocurrent response of g-C3N4 film: the role of thiourea. Applied Surface Science, **2016,** *389*, 1076-1083.

45. Kolesnyk, I.; Kujawa, J.; Bubela, H.; Konovalova, V.; Burban, A.; Cyganiuk, A.; Kujawski, W. Photocatalytic properties of PVDF membranes modified with g-C3N4 in the process of Rhodamines decomposition. Separation and Purification Technology, **2020,** *250*, 117231.

46. Mirzaei, H.; Ehsani, M. H.; Shakeri, A.; Ganjali, M. R.; Badiei, A. Preparation and photocatalytic application of ternary Fe3O4/GQD/g-C3N4 heterostructure photocatalyst for RhB degradation. Pollution, **2022,** *8,3*, 779-791.EHJ HGUQ,DM WFHY

47. Song, X.; Tao, Y.; Liu, J.; Lin, J.; Dai, P.; Wang, Q.; Zheng, CPhotocatalytic-induced bubble-propelled isotropic g-C3N4-coated carbon microsphere micromotors for dynamic removal of organic pollutants. RSC advances, **2022,** 12 ,*21*, 13116-13126.

48. Li, X.; Xiong, J.; Gao, X.; Huang, J.; Feng, Z.; Chen, Z.; Zhu, YRecent advances in 3D g-C3N4 composite photocatalysts for photocatalytic water splitting, degradation of pollutants and CO2 reduction. *Journal of Alloys and Compounds*, **2019,** *802*, 196-209.

49. Kotbi, A.; Imran, M.; Kaja, K.; Rahaman, A.; Ressami, E. M.; Lejeune, M.; Jouiad, M. Graphene and g-C3N4-Based Gas Sensors. *Journal of Nanotechnology*, **2022,** 2022.

50. Hasija, V.; Raizada, P.; Sudhaik, A.; Sharma, K.; Kumar, A.; Singh, P.; Thakur, V. KRecent advances in noble metal free doped graphitic carbon nitride based nanohybrids for photocatalysis of organic contaminants in water: a review. Applied Materials Today, **2019,***15*, 494-524.

51. Niu, P.; Zhang, L.; Liu, G.; Cheng, H. M. Graphene-like carbon nitride nanosheets for improved photocatalytic activities. Advanced Functional Materials, **2012,** *22 ,22*, 4763-4770.

52. Jürgens, B.; Irran, E.; Senker, J.; Kroll, P.; Müller, H.; Schnick, W. Melem (2, 5, 8-triamino-tri-s-triazine), an important intermediate during condensation of melamine rings to graphitic carbon nitride: Synthesis, structure determination by X-ray powder diffractometry, solid-state NMR, and theoretical studies. *Journal of the American Chemical Society*, **2003,** *125 ,34*, 10288-10300.

53. Lotsch, B. V.; Döblinger, M.; Sehnert, J.; Seyfarth, L.; Senker, J.; Oeckler, O.; Schnick, W. Unmasking melon by a complementary approach employing electron diffraction, solid-state NMR spectroscopy, and theoretical calculations—structural characterization of a carbon nitride polymer. *Chemistry–A European Journal*, **2007,** *13 ,17,* 4969-4980.

54. Hong, Y.; Liu, E.; Shi, J.; Lin, X.; Sheng, L.; Zhang, M.; Chen, J. A direct one-step synthesis of ultrathin g-C3N4 nanosheets from thiourea for boosting solar photocatalytic H2 evolution. *international journal of hydrogen energy*, **2019,** *44 ,14,* 7194-7204.

55. Zhou, D.; Qiu, C. Study on the effect of Co doping concentration on optical properties of g-C3N4. Chemical Physics Letters, **2019,** *728,* 70-73.

56. Ye, L.; Liu, J.; Jiang, Z.; Peng, T.; Zan, L. Facets coupling of BiOBr-g-C3N4 composite photocatalyst for enhanced visible-light-driven photocatalytic activity. Applied Catalysis B: Environmental, **2013,** *142*, 1-7.

57. Nguyen, H. P.; Nguyen, T. N.; Lee, S. W.; Hoang, M. H. The use of g-C3N4/MOFs (Fe) as a photocatalyst for remediation of pharmaceutics in water. Materials Research Express. **2022.**

58. Lin, H.; Yang, Y.; Shang, Z.; Li, Q.; Niu, X.; Ma, Y.; Liu, A. Study on the enhanced remediation of petroleum-contaminated soil by biochar/g-C3N4 composites. *International Journal of Environmental Research and Public Health*, **2022,**1*9,14,* 8290.

59. Nasri, M. S. I.; Samsudin, M. F. R.; Tahir, A. A.; Sufian, S. Effect of MXene Loaded on g-C3N4 Photocatalyst for the Photocatalytic Degradation of Methylene Blue. Energies, **2022,** *15,3,* 955.

60. Lökçü, E.; Kaçar, N.; Çayirli, M.; Özden, R. C.; Anik, M. Photoassisted Charging of Li-Ion Oxygen Batteries Using g-C3N4/rGO Nanocomposite Photocatalysts. ACS applied materials interfaces.;**2022.**

61. Su, Y.; Su, L.; Liu, B.; Lin, Y.; Tang, D. Self-powered photoelectrochemical assay for Hg2+ detection based on g-C3N4-CdS-CuO composites and redox cycle signal amplification strategy. Chemosensors**, 2022,** *10,7,* 286.

62. Yuan, X.; Qu, S.; Huang, X.; Xue, X.; Yuan, C.; Wang, S.; Cai, P. Design of core-shelled g-C3N4@ ZIF-8 photocatalyst with enhanced tetracycline adsorption for boosting photocatalytic degradation. *Chemical Engineering Journal* **, 2021**, *416,* 129148.

63. Sun, E.; Wei, H.; Zhang, S.; Bi, Y.; Huang, Z.; Ji, G.; Zhao, C. Adsorption Coupling Photocatalytic Removal of Gaseous n-Hexane by Phosphorus Doped g-C3N4/TiO2/Zn ,OAc) 2-ACF Composites, **2022.**

64. Yang, Z.; Xing, Z.; Feng, Q.; Jiang, H.; Zhang, J.; Xiao, Y.; Zhou, W. Sandwich-like mesoporous graphite-like carbon nitride (Meso-g-C3N4)/WP/Meso-g-C3N4 laminated heterojunctions solar-driven photocatalysts. *Journal of colloid and interface science*, **2020,** *568,* 255-263.

65. Zada, A.; Khan, M.; Hussain, Z.; Shah, M. I. A.; Ateeq, M.; Ullah, M.; Dang, A. Extended visible light driven photocatalytic hydrogen generation by electron induction from g-C3N4 nanosheets to ZnO through the proper heterojunction. Zeitschrift für Physikalische Chemie, **2022,** *236 ,1,* 53-66.

66. Deiminiat, B.; Rounaghi, G. H. A novel visible light photoelectrochemical aptasensor for determination of bisphenol A based on surface plasmon resonance of gold nanoparticles activated g-C3N4 nanosheets. Journal of Electroanalytical Chemistry, **2021,** *886,* 115122.

67. Ma, B.; Zhao, J.; Ge, Z.; Chen, Y.; Yuan, Z. 5 nm NiCoP nanoparticles coupled with g-C3N4 as high-performance photocatalyst for hydrogen evolution. *Science China Materials*,**2020,** *63 ,2,* 258-266.

68. Agha Beygli, R.; Mohaghegh, N.; Rahimi, E. Metal ion adsorption from wastewater by g-C3N4 modified with hydroxyapatite: a case study from Sarcheshmeh acid mine drainage. *Research on Chemical Intermediates*, **2019,** *45,4*, 2255-2268.

69. Mančík, P.; Bednář, J.; Svoboda, L.; Dvorský, R.; Matýsek, D. Photocatalytic reactivation of gC 3 N 4 based nanosorbent. *NANOCON* **,2017**, 289-294.

70. Kroke, E.; Schwarz, M.; Horath-Bordon, E.; Kroll, P.; Noll, B.; Norman, A. D. Tri-s-triazine derivatives. Part I. From trichloro-tri-s-triazine to graphitic structures. *New Journal of Chemistry*, **2002,** *26 ,5*, 508-512.

71. Cook, A. M. Biodegration of s-triazine xenobiotics. FEMS Microbiology Reviews, **1987,***3,2,* 93-116.

72. Hosmane, R. S.; Rossman, M. A.; Leonard, N. J. Synthesis and structure of tri-s-triazine. *Journal of the American Chemical Society*, **1982.** *104 ,20*, 5497-5499.

73. Zhou, X.; Shi, Y.; Xu, W.; Wang, Y.; Zhang, Y.; Wang, Y.; Zhong, W. Ultra-thin deaminated tri-s-triazine-based crystalline nanosheets with high photocatalytic hydrogen evolution performance. *Journal of Alloys and Compounds*, **2020,** *827*, 154307.

74. Rao, M. H.; D GHULE, V. I. K. A. S.; Muralidharan, KNitrogen-rich compounds: s-triazine and tri-s-triazine derivatives as high energy materials. Journal of Chemical Sciences, **2022,** 134.

75. Wang, K.; Li, Q.; Liu, B.; Cheng, B.; Ho, W.; Yu, J.. Sulfur-doped g-C3N4 with enhanced photocatalytic CO2-reduction performance. Applied Catalysis B: Environmental, **2015,***176*, 44-52.